Wafer-scale silicon nanopillars and nanocones by Langmuir–Blodgett assembly and etching

Ching-Mei Hsu,[1] Stephen T. Connor,[2] Mary X. Tang,[3] and Yi Cui[1,a)]
[1]*Department of Materials Science and Engineering, Stanford University, Stanford, California 94305, USA*
[2]*Department of Chemistry, Stanford University, Stanford, California 94305, USA*
[3]*Stanford Nanofabrication Facility, Stanford, California 94305, USA*

(Received 13 August 2008; accepted 30 August 2008; published online 1 October 2008)

We have developed a method combining Langmuir–Blodgett assembly and reactive ion etching to fabricate nanopillars with uniform coverage over an entire 4 inch wafer. We demonstrated precise control over the diameter and separation between the nanopillars ranging from 60 to 600 nm. We can also change the shape of the pillars from having vertical to tapered sidewalls with sharp tips exhibiting a radius of curvature of 5 nm. This method opens up many possible opportunities in nanoimprinting, solar cells, batteries, and scanning probes. © *2008 American Institute of Physics*. [DOI: 10.1063/1.2988893]

Vertical arrays of nanopillars, nanowires, or nanocones have been sought after for many applications. For example, vertical Si nanopillars with aspect ratios less than 5 have been used as nanoimprint masters.[1] Vertical nanowire arrays of larger aspect ratios have also been exploited in solar cells[2] and vertical field effect transistors.[3] A tapered geometry in vertical nanocone arrays has been shown to be beneficial for the reduction in light reflection via refractive index matching[4] and will also afford new structures as scanning probe tips. Recently, we demonstrated that Si and Ge nanowires could serve as ultrahigh charge storage capacity Li-ion battery negative electrodes.[5] We believe that vertical arrays of nanowires, nanopillars, or nanocones may improve battery performance. For many of these applications, the diameter, spacing, and shape of the vertical nanostructures need to be precisely controlled. All of these arrays should be fabricated over a large area with high throughput and low cost.

Several methods have been used to fabricate vertical arrays. Nanowire arrays have been synthesized using the vapor-liquid-solid method with high diameter control;[6] however, obtaining small separation between nanowires has been challenging due to the merging of metal catalyst particles at growth temperatures. Nanowire arrays have been made using solution chemistry, although the control of spacing and diameter is limited.[7] Electron-beam lithography combined with etching can define features down to sub-10 nm,[8] but the cost is high and the throughput is low. Photolithography is a possible choice, although the cost is too high for many applications. Recently, a technique known as natural lithography[9] has exploited arrays of chemically synthesized nanospheres as masks for patterning different shapes of particles and pillars.[10] The advantage of this approach is that nanospheres can assemble into close-packed arrays. The spacing and diameter can then be tuned with nanoscale control by etching. Spin coating is usually used to prepare single or multiple layers of nanospheres. While spin coating is quick and cost-effective,[11] the resulting monolayer of nanospheres is not close packed and does not cover a large area but rather forms domains. The Langmuir–Blodgett (LB) method is known as a reliable technique to prepare a monolayer of nanoparticles over a large area,[12] yet it has not been used for controlled nanopillar/nanocone formation. Herein, we exploit LB assembled nanoparticles as a mask for reactive ion etching (RIE) to fabricate nanopillars with uniform coverage over an entire 4 inch wafer. We demonstrate precise control over a wide range of diameters and spacings. We can also tune the shape from vertical pillars to nanocones, which have sharp tips with radius of curvature of 5 nm.

Figure 1 shows the general fabrication process for making the Si nanopillars. First, monodisperse SiO_2 nanoparticles, synthesized in-house, were assembled into a close-packed monolayer on a Si ⟨100⟩ wafer using the LB method [Fig. 1(a)]. Monodisperse SiO_2 particles with diameters from 50 to 800 nm were produced by a modified Stöber synthesis.[13] Before LB assembly, SiO_2 particles were modi-

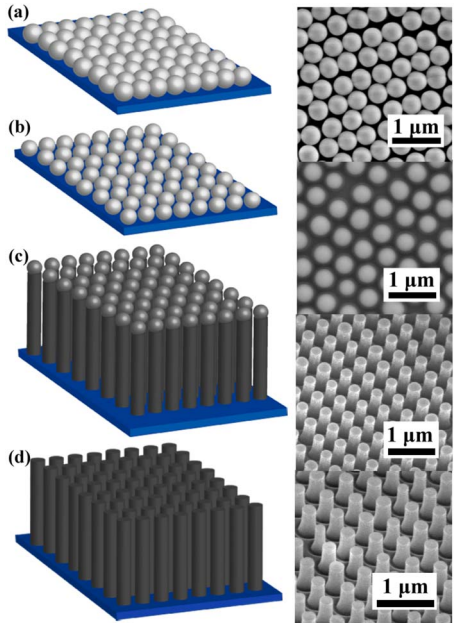

FIG. 1. (Color online) Fabrication process of Si nanopillars. (a) Deposition of the silica nanoparticles by LB. (b) Shrinking of the mask by isotropic RIE of SiO_2. (c) Anisotropic etching of Si into pillars by RIE. (d) Removal of the residual mask by HF etching.

a)Author to whom correspondence should be addressed. Electronic mail: yicui@stanford.edu.

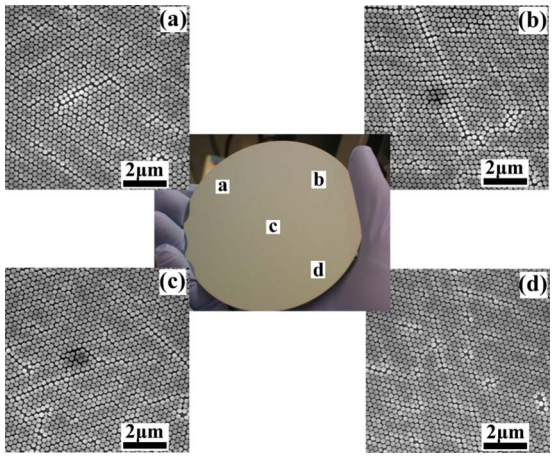

FIG. 2. (Color online) (a)–(d) are SEM images of randomly selected areas at great distances from each other on a 4 inch wafer with nanoparticles deposited by LB.

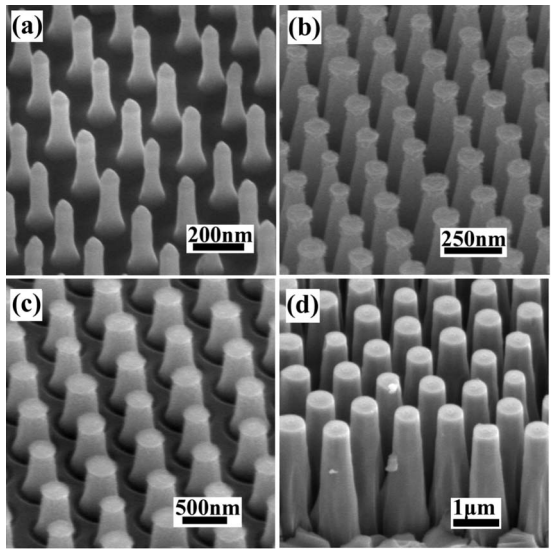

FIG. 3. SEM images of nanopillar arrays with uniform tip diameters of (a) 60, (b) 125, (c) 300, and (d) 600 nm.

fied with aminopropyl methyldiethoxysilane so as to terminate them with positively charged amine groups and prevent aggregation. Second, the diameter and spacing of the nanoparticles were tuned by selective and isotropic RIE of SiO_2 [Fig. 1(b)]. The etching is based on fluorine chemistry using a mixture of O_2 and CHF_3. This shrinking step also removed the native oxide from the Si substrate, facilitating further etching. Third, Si nanopillars were formed by Cl_2 based selective and anisotropic RIE of the Si substrate [Fig. 1(c)]. The diameter and spacing of the nanopillars were determined by the initial nanoparticle size and both SiO_2 and Si etching times. Finally, SiO_2 particles at the tips of pillars can be selectively removed by etching with hydrofluoric acid (HF) [Fig. 1(d)].

One important characteristic of our approach is that hexagonal, close-packed monolayers of nanoparticles can be produced on a wafer-scale within the short 60 min LB assembly and deposition. Figure 2 shows a digital camera picture of a 4 inch wafer covered by a monolayer of 200 nm diameter SiO_2 particles. Scanning electron microscope (SEM) images at four random locations far from each other show that a monolayer of particles covers the whole wafer. Although line and point defects exist in the nanoparticle packing, we did not observe any area that was not covered by the nanoparticles.

Using this method, the entire area covered with nanoparticles was transformed into nanopillars. Experiments were performed to demonstrate control over the nanopillar diameter and spacing. In the first series, samples starting with nanoparticle diameters slightly larger than the desired pillar diameters were etched isotropically to between 120 and 600 nm. The resulting nanopillars with corresponding diameters can be seen in Figs. 3(b)–3(d). Pillars with diameters less than 100 nm were obtained through a combination of thermal oxidation of large Si nanopillars and HF etching. Figure 3(a) shows nanopillars with 60 nm diameters. When nanoparticle diameters are sub-100 nm, the spacing between nanoparticles decreases proportionately. This restricts ionic and reactive neutral species from arriving on the silicon surface during RIE and also impedes byproduct removal.[14] Therefore, the aforementioned silicon oxidation technique was used to evenly decrease the final nanopillar diameter over the whole wafer. In the second series, represented in Fig. 4, nanopillars of varying spacings from 50 to 400 nm were fabricated by etching nanoparticles with diameters of 200 to 500 nm. Nanopillar arrays with desired diameter (D) and spacing (S) can be rationally designed. Since the center-to-center distance of neighboring nanopillars is $D+S$, the SiO_2 nanoparticles can be chosen to have an initial diameter of $D+S$ and

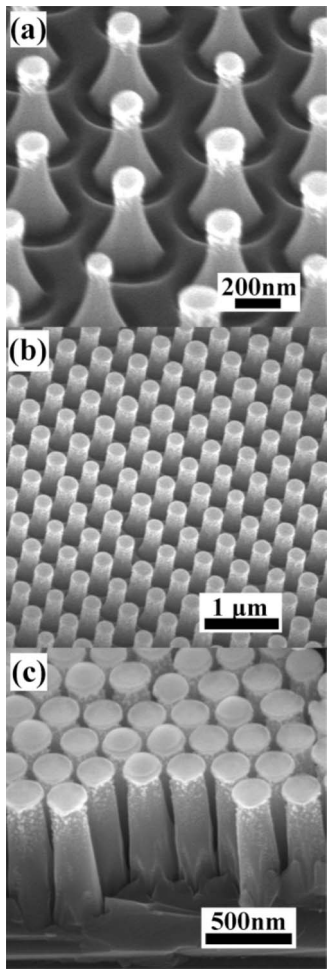

FIG. 4. Nanopillar arrays with a spacing of (a) 400, (b) 350, and (c) 50 nm.

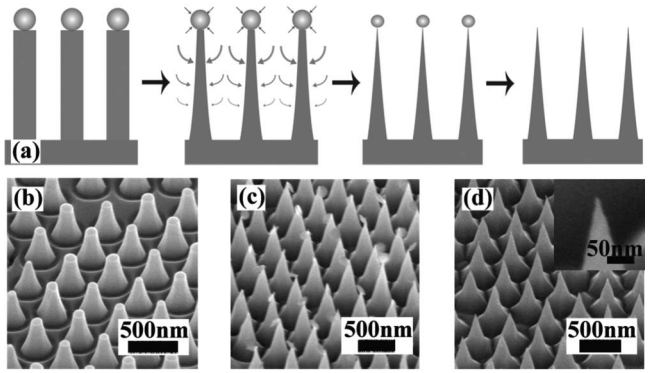

FIG. 5. (a) Schematic of sharpening process with thicker arrows indicating faster etching rate. (b)–(d) show SEM images corresponding to intermediate and final steps, with inset in (d) of a tip.

be etched by $\frac{1}{2}S$. The diameter of the initial nanoparticles can be precisely controlled from 50 to 800 nm. RIE etching can be controlled with an accuracy of ~10 nm. Thus, we have precise control of the nanopillar diameter and spacing over a wide range, which is particularly suitable for applications in solar cells and batteries.

Tapering was present in most of our nanopillar samples for several reasons. First, Cl and Br free radicals arrive at the Si surface from all directions during RIE, inducing some isotropic etching of Si or undercutting during the supposedly anisotropic steps. Second, the etching selectivity of Si to SiO_2 is around 26; therefore, the extent of lateral etching will increase due to mask erosion when using SiO_2 masks. Third, when the etched products are deposited during etching, tapered sidewalls can occur since the deposition rate decreases from the bottom to the top of the pillar.

However, the undercutting can be utilized to form unique, sharp nanocones through control of the etching conditions. The idea is as follows [Fig. 5(a)]. First, Si nanopillars were formed by Cl_2 based anisotropic RIE. Second, C_2ClF_5/SF_6 was used for further isotropic etching of preformed nanopillars, which created undercut and sharpened the nanopillars.[15] Figures 5(b)–5(d) show the SEM images at different stages of the sharpening process. Accompanying the sharpening is the shrinkage of the SiO_2 spheres [Fig. 5(c)]. Excitingly, the combination of anisotropic and isotropic etching can lead to a sharpening of the tips to a radius of curvature of 5 nm [Fig. 5(d)], opening up the opportunities for refractive index matching and array-based high resolution probes.

In conclusion, we have developed a method to produce close-packed arrays of Si nanopillars over an entire 4 in. wafer by the synergy of LB deposition and etching. We demonstrated unprecedented control of the diameters and spacings over a wide range. We also tuned the shape of the pillars from having vertical to tapered sidewalls, allowing for sharp nanotips with a radius of curvature of 5 nm.

This work is supported by the Stanford Global Climate and Energy Project, the Center for Cancer Nanotechnology Excellence Focused on Therapy Response and the U. S. Office of Naval Research. S.T.C. acknowledges support from a National Science Foundation Graduate Fellowship. Ching-Mei Hsu and Stephen T. Connor contributed equally to this work.

[1] S. Y. Chou, P. R. Krauss, and P. J. Renstrom, Science **272**, 85 (1996).
[2] M. Law, L. E. Greene, J. C. Johnson, R. Saykally, and P. Yang, Nat. Mater. **4**, 455 (2005); M. D. Kelzenberg, D. B. Turner-Evans, B. M. Kayes, M. A. Filler, M. C. Putnam, N. S. Lewis, and H. A. Atwater, Nano Lett. **8**, 710 (2008).
[3] J. Goldberger, A. I. Hochbaum, R. Fan, and P. Yang, Nano Lett. **6**, 973 (2006); P. Nguyen, H. T. Ng, T. Yamada, M. K. Smith, J. Li, J. Han, and M. Meyyappan, *ibid.* **4**, 651 (2004); T. Bryllert, L. E. Wernersson, L. E. Froberg, and L. Samuelson, IEEE Electron Device Lett. **27**, 323 (2006).
[4] Y.-F. Huang, S. Chattopadhyay, Y.-J. Jen, C.-Y. Peng, T.-A. Liu, Y.-K. Hsu, C.-L. Pan, H.-C. Lo, C.-H. Hsu, Y.-H. Chang, C.-S. Lee, K.-H. Chen, and L.-C. Chen, Nat. Nanotechnol. **2**, 770 (2007).
[5] C. K. Chan, H. L. Peng, G. Liu, K. McIlwrath, X. F. Zhang, R. A. Huggins, and Y. Cui, Nat. Nanotechnol. **3**, 31 (2008); C. K. Chan, X. F. Zhang, and Y. Cui, Nano Lett. **8**, 307 (2008).
[6] Y. Cui, L. J. Lauhon, M. S. Gudiksen, J. F. Wang, and C. M. Lieber, Appl. Phys. Lett. **78**, 2214 (2001); A. I. Hochbaum, R. He, R. Fan, and P. Yang, Nano Lett. **5**, 457 (2005).
[7] L. E. Greene, M. Law, D. H. Tan, M. Montano, J. Goldberger, G. Somorjai, and P. Yang, Nano Lett. **5**, 1231 (2005).
[8] W. Chen and H. Ahmed, Appl. Phys. Lett. **63**, 1116 (1993).
[9] H. W. Deckman and J. H. Dunsmuir, Appl. Phys. Lett. **41**, 377 (1982); J. C. Hulteen and R. P. Vanduyne, J. Vac. Sci. Technol. A **13**, 1553 (1995).
[10] K. Seeger and R. E. Palmer, J. Phys. D **32**, L129 (1999); K. Peng, M. Zhangf, A. Lu, N.-B. Wong, R. Zhang, and S.-T. Lee, Appl. Phys. Lett. **90**, 163123 (2007).
[11] P. Jiang, T. Prasad, M. J. McFarland, and V. L. Colvin, Appl. Phys. Lett. **89**, 011908 (2006); P. Jiang and M. J. McFarland, J. Am. Chem. Soc. **126**, 13778 (2004).
[12] C. P. Collier, R. J. Saykally, J. J. Shiang, S. E. Henrichs, and J. R. Heath, Science **277**, 1978 (1997); B. O. Dabbousi, C. B. Murray, M. F. Rubner, and M. G. Bawendi, Chem. Mater. **6**, 216 (1994); M. Sastry, in *Colloids and Colloid Assemblies*, edited by F. Caruso (Wiley, Weinheim, 2004), p. 369.
[13] G. H. Bogush, M. A. Tracy, and C. F. Zukoski, J. Non-Cryst. Solids **104**, 95 (1988).
[14] J. D. Plummer, M. D. Deal, and P. B. Griffin, *Silicon VLSI Technology-Fundamentals, Practice and Modeling* (Prentice-Hall, Upper Saddle River, 2000).
[15] J. P. McVittie and C. Gonzales, Presented at the Fifth Symposium on Plasma Processing, the Electrochemical Society, 1985 (unpublished).